Development and Validation of a Quantitative LCMS/MS Method for Measuring CYP4V2 Enzyme Activity in rAAV-hCYP4V2 Gene Therapy Products

Ge Ren , Qin Xi , Yiran Li , Wenjing Luo , Yanrong Cao , Yong Zhou * , Chenggang Liang *

Posted Date: 24 March 2026

doi: 10.20944/preprints202603.1833.v1

Keywords: LC-MS/MS; CYP4V2; enzyme activity; AAV; gene therapy; lauric acid ω-hydroxylation; method validation

 doi:10.20944/preprints202603.1833.v1

Article

Development and Validation of a Quantitative LC-MS/MS Method for Measuring CYP4V2 Enzyme Activity in rAAV-hCYP4V2 Gene Therapy Products

Ge Ren [1,2,3,†], Xi Qin [1,2,†], Yiran Li [1,2,†], Wenjing Luo [4], Yanrong Cao [4], Yong Zhou [1,2,*] and Chenggang Liang [1,2,*]

[1] National Institutes for Food and Drug Control, 100050 Beijing, China
[2] State Key Laboratory of Drug Regulatory Science, 100050 Beijing, China
[3] School of Life and Health Sciences, Hubei University of Technology, 430068 Wuhan, China
[4] Shanghai Vitalgen BioPharma Co., Ltd., Shanghai 201210, China
* Correspondence: zhouyong@nifdc.org.cn (Y.Z.); liangchenggang@nifdc.org.cn (C.L.)
† These authors contributed equally to this work.

Abstract

Bietti crystalline dystrophy (BCD) is a hereditary retinal disease caused by loss-of-function mutations in the CYP4V2 gene. Gene replacement therapy using rAAV-hCYP4V2 represents a promising therapeutic strategy, requiring robust bioassays for product quality control. This study developed and validated a sensitive LC-MS/MS method for quantifying CYP4V2 enzyme activity. Lysates from HeLa-AAVR cells transduced with rAAV-hCYP4V2 (MOI=3×10^5) were used, with lauric acid as substrate supplemented with cytochrome P450 reductase, cytochrome b5, and NADPH. The ω-hydroxylated product (12-hydroxy lauric acid) was quantified using tolbutamide as internal standard. Method validation followed ICH guidelines. Results demonstrated excellent specificity with negligible background in negative controls. Linearity was achieved over 0.5-100 ng/mL (R^2>0.99), with average recovery of 100.6%. Intra-batch and inter-batch precision RSDs were <47.8% and <28.4%, respectively. Product stability was maintained ≥4 weeks at -80℃. The method was successfully applied to three AAV serotypes (AAV2, AAV8, AAV2/8), with all RSDs <23.9%. This validated LC-MS/MS bioassay provides a crucial quality control tool for potency assessment, process development, batch release, and stability studies of rAAV-hCYP4V2 gene therapy products.

Keywords: LC-MS/MS; CYP4V2; enzyme activity; AAV; gene therapy; lauric acid ω-hydroxylation; method validation

1. Introduction

Bietti crystalline dystrophy (BCD) is an autosomal recessive hereditary retinal degenerative disease.[1–3] Its pathological characteristics include the presence of shiny yellow crystalline deposits in the retinal pigment epithelium (RPE) and choroid,[4] accompanied by progressive atrophy of RPE and photoreceptor cells, which can ultimately lead to visual field defects, night blindness, and loss of central vision.[5] Molecular genetic studies have shown that BCD is primarily caused by loss-of-function mutations in the *CYP4V2* gene. This gene encodes the CYP4V2 enzyme, a member of the cytochrome P450 superfamily, whose primary physiological function is to catalyze the ω-hydroxylation of medium- and long-chain fatty acids, including palmitic acid and lauric acid.[6] Inactivation of the CYP4V2 enzyme can obstruct fatty acid metabolism, triggering abnormal lipid accumulation, oxidative stress, and ferroptosis,[7] ultimately resulting in irreversible damage to RPE cells. Currently, there is no approved, effective therapy for BCD, resulting in a significant unmet clinical need.[8]

 doi:10.20944/preprints202603.1833.v1

Gene replacement therapy using adeno-associated virus (AAV) vectors offers a promising therapeutic approach for BCD.[9] rAAV-hCYP4V2 is a gene therapy under development product based on AAV vectors, designed to deliver the functional *CYP4V2* gene to retinal cells via a single administration, thereby restoring enzyme function and delaying or preventing disease progression. Currently, three products (NCT06302608, NCT04722107, and NCT05694598) are undergoing clinical trials, all of which have shown significant progress.[2,8,10] To ensure the batch-to-batch consistency, potency, and effectiveness of such biological products during production and quality control, it is crucial to establish a precise, stable, and quantifiable method for assessing biological activity.[11]

At present, commonly used CYP450 enzyme activity assays, such as *in vitro* tissue homogenization and fluorescence-based methods, suffer from limitations including indirect inference, susceptibility to matrix interference, or insufficient specificity for distinguishing target enzyme activity. Thus, they fail to meet the requirements for efficient potency determination of gene therapy products.[12–14] Due to its high sensitivity, specificity, and excellent quantitative performance, liquid chromatography-mass spectrometry (LC-MS/MS) has become the gold standard for quantifying low-concentration small-molecule metabolites in complex biological matrices. However, no systematically optimized and comprehensively validated LC-MS/MS method is currently available for quantifying CYP4V2 enzyme activity in rAAV-hCYP4V2 gene therapy products that can be directly used for product quality control and release.

Therefore, this study aims to establish and validate an LC-MS/MS-based CYP4V2 enzyme activity assay to directly, specifically, and quantitatively evaluate the functional activity of the rAAV-hCYP4V2. This method utilizes lauric acid as the substrate, and the enzymatic catalytic activity is reflected by the generated ω-hydroxylation product (12-hydroxy lauric acid). Systematic optimization and comprehensive validation of the method were performed to ensure compliance with the technical requirements for biological product activity determination specified in the Pharmacopoeia of the People's Republic of China and relevant international guidelines. The developed method represents a reliable analytical tool for the research, development, and quality control of rAAV-hCYP4V2 products.

2. Results

2.1. Exploration of the Enzymatic Reaction System: Establishment of the System from Intracellular to Extracellular Reaction

In the early stages of the study, we added substrates directly to FreeStyle 293 or ARPE-19 cells transfected with BCD plasmids to initiate the reaction; however, no reaction products were detected (concentrations below the lower limit of quantification (LLOQ)). This indicates that substrate accessibility or endogenous metabolic interference may limit reaction efficiency in intact cells. Therefore, the research strategy was shifted to an extracellular reaction system, in which cell lysate was used as the enzyme source to reconstruct an *in vitro* reaction environment containing all necessary cofactors.

Preliminary experiments revealed that when lysates from 293 cells transfected with the BCD plasmid were used, and excess cytochrome P450 reductase (40 nM) and cytochrome b5 (20 nM) were added, the product 12-hydroxylauric acid could be successfully detected using 250 μM lauric acid as the substrate. The yield of this product showed a good linear relationship with reaction time over 90 min (R^2 = 0.9697). This result confirms the feasibility of the extracellular reaction strategy and highlights the crucial role of cofactor saturation in enabling the CYP4V2 enzyme to reach its maximum catalytic rate. Based on this finding, the core reaction conditions for subsequent method development were defined as follows: cell lysate as the enzyme source, and an optimized reaction system containing 40 nM P450 reductase, 20 nM cytochrome b5, and 250 μM lauric acid.

 doi:10.20944/preprints202603.1833.v1

2.2. Optimization of cell Models and Virus Transduction Conditions

2.2.1. Exploration of MOI in Viral Transduction

Virus transduction was performed in HEK293 cells seeded at a density of 3×10^6 cells, and enzyme activity was assessed at reaction times of 0, 30, 60, and 90 min. When the MOI was 3×10^5, the linear relationship between enzymatic reaction and time was most pronounced, and the highest relative enzyme activity was observed (Figure 1). Therefore, this MOI value was selected for subsequent optimization.

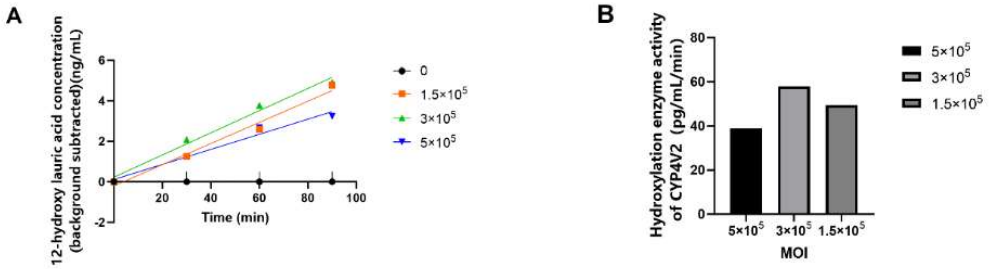

Figure 1. (A) Changes in product concentration over time (0 to 90 min) following rAAV-hCYP4V2 transduction in HEK293 cells at different MOIs. (B) CYP4V2 hydroxylase activity in HEK293 cells transduced with rAAV-hCYP4V2 at different MOIs over 0 to 90 min.

2.2.2. Optimization of Cell Types

To further improve viral transduction efficiency, HeLa-AAVR cells overexpressing the AAV receptor were used. Comparative experiments revealed that CYP4V2 enzyme activity was significantly higher in cells pretreated with 0.5 mM hydroxyurea (HU) than that in cells without HU pretreatment or in HEK293 cells pretreated with 0.5 mM HU (Figure 2A). Therefore, the standard condition was defined as HeLa-AAVR cells pre-treated with 0.5 mM HU for 24 h. Meanwhile, experimental results (Table 1) showed that the reaction products could be detected during the enzyme activity assay over a period of 0-120 min. Product concentration increased with reaction time from 0 to 45 min, showing a good linear relationship (Figure 2B). Thus, in subsequent experiments, the enzymatic reaction was controlled within 45 min.

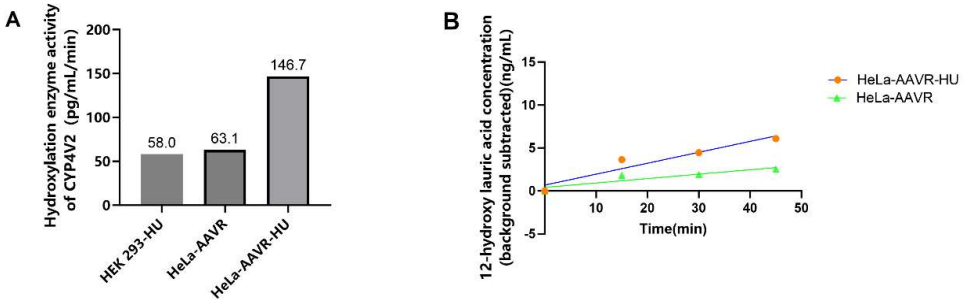

Figure 2. (A) CYP4V2 hydroxylase activity following rAAV-hCYP4V2 transduction in HEK293 and HeLa-AAVR cells. (B) Changes in product concentration over time following rAAV-hCYP4V2 transduction in HeLa-AAVR cells.

 doi:10.20944/preprints202603.1833.v1

Table 1. Product concentration in enzymatic reactions after rAAV-hCYP4V2 transduction in HeLa-AAVR cells.

Product name	HU=0			HU=0.5 mM		
	Time (min)	Product concentration (ng/mL)	Product concentration after background subtraction (ng/mL)	Time (min)	Product concentration (ng/mL)	Product concentration after background subtraction (ng/mL)
12-Hydroxylauric acid	0	4.17	0	0	3.33	0
	15	6	1.83	15	6.97	3.64
	30	6.07	1.9	30	7.78	4.45
	45	6.71	2.54	45	9.42	6.09
	60	5.51	1.34	60	9.44	6.11
	75	5.21	1.04	75	4.17	0.84
	90	5.38	1.21	90	5.81	2.48
	105	3.22	-0.95	105	9.11	5.78
	120	4.79	0.62	120	10.11	6.78

2.2.3. Matrix Screening for Optimal Viral Transduction Conditions

To further determine the optimal viral transduction conditions, product concentration was measured using a matrix experiment (cell seeding numbers: 1 x 10^6, 3 x 10^6, and 5 x 10^6; MOI: 3 x 10^4, 1 x 10^5, and 3 x 10^5) combined with an endpoint assay (reaction time: 45 min). The results showed that the highest enzyme activity (269.3 pg/mL/min) was achieved at a cell seeding number of 3 x 10^6 and an MOI of 3 x 10^5 (Figure 3, Table 2), which were therefore selected as the optimal transduction conditions. It should be noted that after background subtraction, some combinations (e.g., low MOI or high cell density) resulted in calculated negative enzyme activity values (e.g., -8.87 pg/mL/min). These negative values are a mathematical result of minor signal fluctuations around the background level or when the measured signal falls below the lower limit of quantification (LLOQ). They do not represent actual negative enzymatic activity but rather indicate that the product concentration was indistinguishable from the background noise under these suboptimal transduction conditions.

Table 2. Product concentration and corresponding enzyme activity under different combinations of cell seeding number and MOI.

No.	HeLa-AAVR cell seeding number	Virus MOI	Product concentration at 0 min after enzymatic reaction (ng/mL)	Product concentration at 45 min after enzymatic reaction (ng/mL)	Background subtraction (ng/mL)	Corresponding enzyme activity (pg/mL/min)
1	1.00E+06	3.00E+04	4.01	4.31	0.3	6.67
2	1.00E+06	1.00E+05	3.96	-0.03	-3.99	-88.67
3	1.00E+06	3.00E+05	4.49	5.9	1.41	31.33
4	3.00E+06	3.00E+04	4.72	7	2.28	50.67
5	3.00E+06	1.00E+05	5.33	14.01	8.68	192.89
6	3.00E+06	3.00E+05	6.01	18.12	12.11	269.11
7	5.00E+06	3.00E+04	7.4	7.23	-0.17	-3.78
8	5.00E+06	1.00E+05	5.63	13.72	8.09	179.78
9	5.00E+06	3.00E+05	6.02	14.71	8.69	193.11

 doi:10.20944/preprints202603.1833.v1

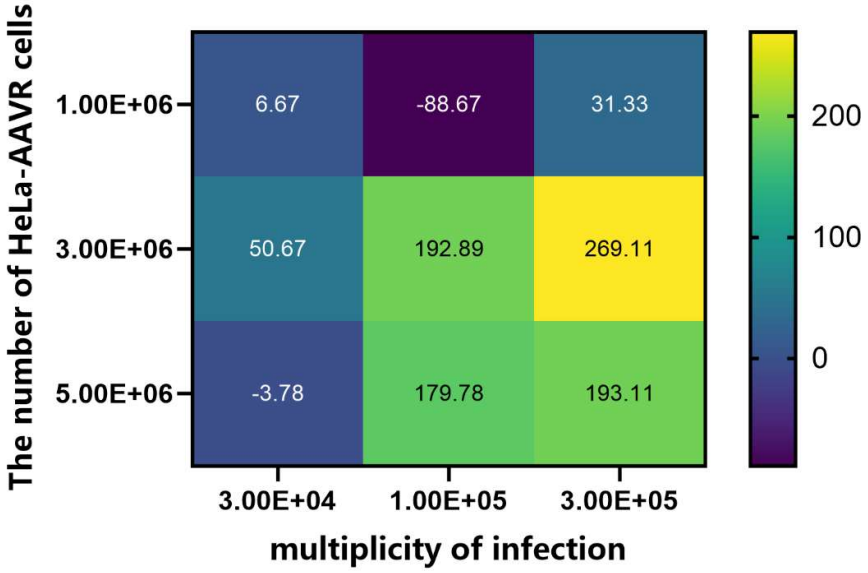

Figure 3. CYP4V2 hydroxylase activity detected by end point method under different combinations of cell seeding number and MOI.

2.2.4. Confirmation of Enzyme Activity Reaction Time Points

The optimal time points for the enzymatic reaction were determined among 0, 5, 15, 25, 35, 45, 55, 65, 90, and 120 min. As shown in Figure 4, the product concentration reached its maximum at 35 min and exhibited a good linear relationship over the 0-35 min interval, after which the product concentration began to decrease (Table 3). Therefore, 0, 5, 15, 25, and 35 min were selected as the optimal time points for subsequent enzymatic reaction assays.

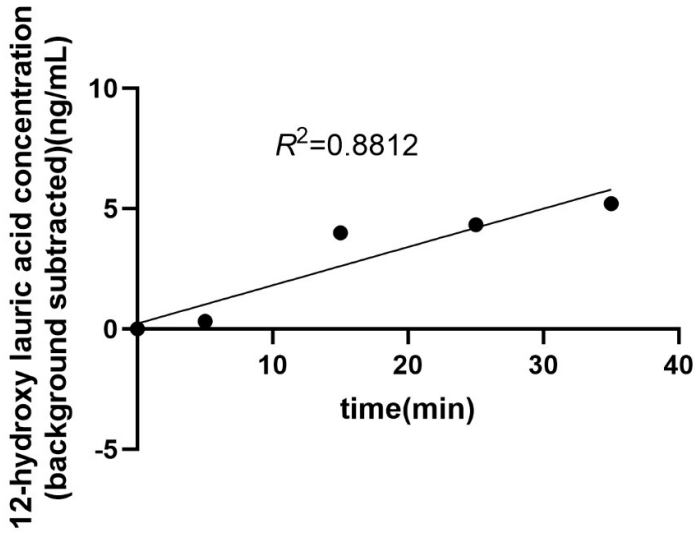

Figure 4. Concentrations of 12-hydroxylauric acid detected at different enzymatic reaction times (0-35 min).

 doi:10.20944/preprints202603.1833.v1

Table 3. Concentrations of 12-hydroxylauric acid detected at different enzymatic reaction times.

reaction time (min)	Product concentration after background subtraction (ng/mL)
0	0
5	0.32
15	3.99
25	4.33
35	5.21
45	3.28
55	3.64
65	4.75
90	4.65
120	5.33

2.3. Optimization of the LC-MS/MS Detection Method

During the early stage of method development, methanol was used for standard curve preparation, and quantification was performed using the external standard method. This approach resulted in high background signals and substantial data fluctuation, indicative of a pronounced solvent effect. Subsequently, standard curve preparation was optimized using a blank matrix, specifically, blank cell lysate without viral transduction, and samples were pre-treated simultaneously. Tolbutamide was then introduced as an internal standard, and quantification was performed using the internal standard method. The optimized method significantly improved assay reproducibility and accuracy.

Under the optimized LC-MS/MS conditions, both 12-hydroxylauric acid and the internal standard produced sharp, symmetrical chromatographic peaks with good separation. The established calibration curve showed good linearity over the concentration range of 0.5-100 ng/mL (R^2>0.99), with an LLOQ of 0.5 ng/mL, fully meeting the quantitative requirements for enzymatic reaction products. Figures 5 and 6 show the calibration curve and representative spectra of 12-hydroxylauric acid and tolbutamide, respectively.

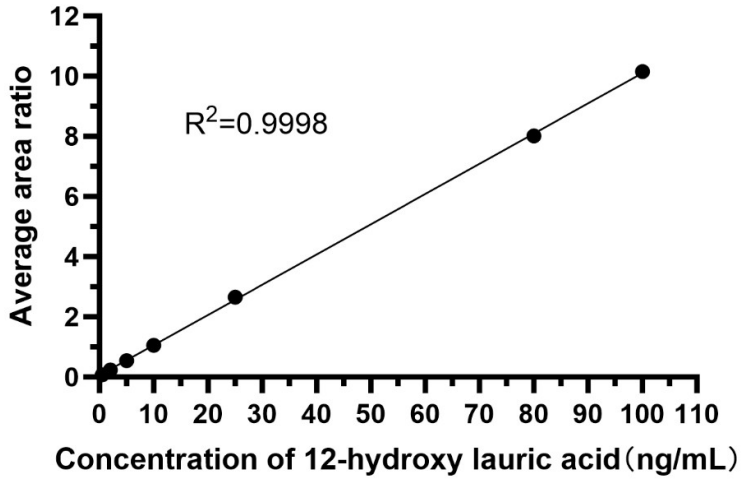

Figure 5. LC-MS/MS calibration curve.

 doi:10.20944/preprints202603.1833.v1

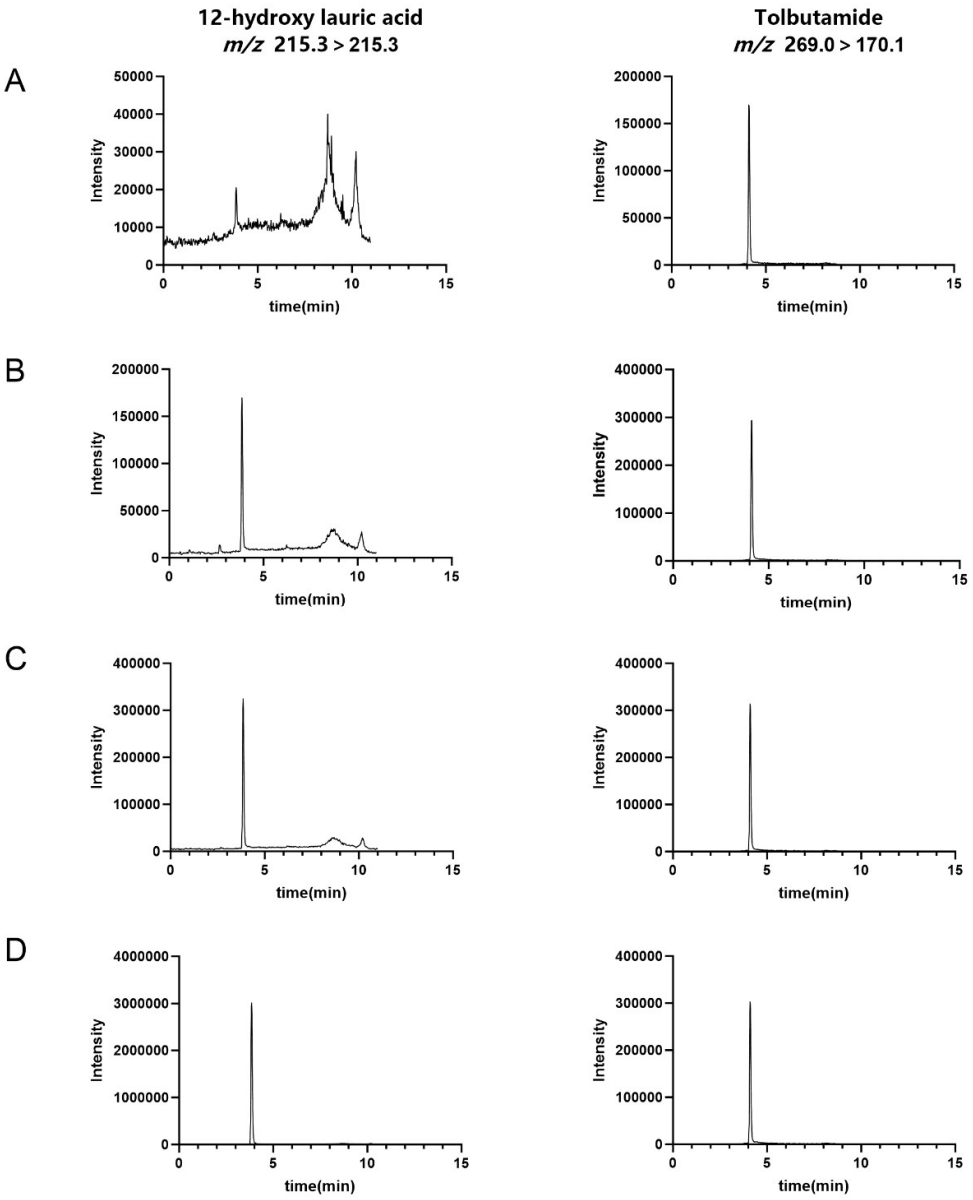

Figure 6. Representative LC-MS/MS spectra of 12-hydroxylauric acid and tolbutamide. (A) A sample containing 0.5 ng/mL 12-hydroxylauric acid (LLOQ), (B) a standard sample containing 5 ng/mL 12-hydroxylauric acid, (C) a standard sample containing 10 ng/mL 12-hydroxylauric acid, and (D) a standard sample containing 100 ng/mL 12-hydroxylauric acid. Demonstrative chromatograms showing the quantification ions of 12-hydroxylauric acid and tolbutamide (internal standard).

2.4. Method Validation and Application Outcomes

2.4.1. Specificity

As shown in Table 4, the product concentrations in both the blank control group and the substrate (acetic acid) group were below the LLOQ. The highest product concentration was observed in the positive group (5.46 ng/mL after background subtraction), corresponding to an enzyme activity of 150.2±9.430 pg/mL/min. The RSD within groups was 6.28%.

 doi:10.20944/preprints202603.1833.v1

Table 4. Specificity evaluation results.

Experimental group	Replicate	Time (min)	Concentration of 12-hydroxylauric acid after background subtraction (ng/mL)	Enzyme activity (pg/mL/min)
Blank control group	Dish 1	0	0.00	NA
		5	-1.55	
		15	-1.56	
		25	-1.39	
		35	-1.34	
	Dish 2	0	0.00	NA
		5	0.23	
		15	0.06	
		25	0.00	
		35	0.12	
	Dish 3	0	0.00	NA
		5	0.00	
		15	0.00	
		25	0.75	
		35	0.56	
Substrate (acetic acid) group	Dish 4	0	0.00	NA
		5	0.00	
		15	0.00	
		25	0.00	
		35	0.59	
	Dish 5	0	0.00	NA
		5	0.00	
		15	0.00	
		25	0.00	
		35	0.00	
	Dish 6	0	0.00	NA
		5	0.00	
		15	0.00	
		25	0.52	
		35	0.52	
Positive control group	Dish 7	0	0.00	147.6
		5	0.85	
		15	2.12	
		25	4.14	
		35	4.87	
	Dish 8	0	0.00	160.7
		5	0.96	
		15	2.21	
		25	4.41	
		35	5.41	
	Dish 9	0	0.00	142.4
		5	0.75	
		15	2.45	
		25	2.70	
		35	5.46	

 doi:10.20944/preprints202603.1833.v1

2.4.2. Accuracy

According to the operation procedure, assuming the measured concentrations were x1 and x2, accuracy was calculated using the following formula: $\{100+\frac{2x2-x1-QC}{x1+QC}\}\times100\%$. As shown in Table 5, spiked recovery accuracy ranged from 87.3% to 106.1%, with an average accuracy of 100.6% and a standard deviation of 6.045.

Table 5. Accuracy evaluation results.

Replicate	Time (min)	Concentration of 12-hydroxylauric acid (ng/mL)	Spiked concentration (ng/mL)	Theoretical concentration (ng/mL)	Measured concentration (ng/mL)	Accuracy %
Dish 1	0	0.56	75.00	37.78	33.00	87.3
	15	2.68	30.00	16.34	17.34	106.1
	35	5.43	1.50	3.465	3.57	103.0
Dish 2	0	0.62	75.00	37.81	39.03	103.2
	15	2.83	30.00	16.415	16.98	103.4
	35	6.03	1.50	3.765	3.63	96.4
Dish 3	0	0.58	75.00	37.79	36.57	96.8
	15	3.03	30.00	16.515	17.38	105.2
	35	6.04	1.50	3.77	3.92	104.0

2.4.3. Precision

Repeatability results are summarized in Table 7, with an RSD of 47.78% calculated from six replicates. Intermediate precision was determined by two operators who measured enzyme activity from three different virus batches over 2 days. The results are shown in Table 6 and Table 7, with an RSD of 28.44% (dish 7 - 15).

Table 6[1]. Repeatability evaluation results.

Replicate	Time (min)	Concentration of 12-hydroxylauric acid after background subtraction (ng/mL)	Enzyme activity (pg/mL/min)
Dish 1	0	0.00	147.6
	5	0.85	
	15	2.12	
	25	4.14	
	35	4.87	
Dish 2	0	0.00	160.7
	5	0.96	
	15	2.21	
	25	4.41	
	35	5.41	
Dish 3	0	0.00	142.4
	5	0.75	
	15	2.45	
	25	2.70	
	35	5.46	
Dish 4	0	0.00	67.2
	5	0.00	
	15	0.95	
	25	1.66	
	35	2.44	

 doi:10.20944/preprints202603.1833.v1

Replicate	Time (min)	Concentration of 12-hydroxylauric acid after background subtraction (ng/mL)	Enzyme activity (pg/mL/min)
Dish 5	0	0.00	52.0
	5	0.52	
	15	0.85	
	25	1.19	
	35	1.83	
Dish 6	0	0.00	60.0
	5	0.51	
	15	0.82	
	25	1.39	
	35	2.18	
Dish 7 Operator B	0	0.00	182.5
	5	0.80	
	15	2.63	
	25	4.55	
	35	6.46	
Dish 8 Operator B	0	0.00	174.5
	5	0.79	
	15	2.61	
	25	4.48	
	35	6.04	
Dish 9 Operator B	0	0.00	184.6
	5	0.99	
	15	2.68	
	25	4.63	
	35	6.48	

Note 1: The three dishes were grouped, and the cell passages used were P16, P20, and P19, respectively. All virus samples were from batch V1.

Table 7[2]. Intermediate precision evaluation results.

Replicate group	Time (min)	Concentration of 12-hydroxylauric acid after background subtraction (ng/mL)	Enzyme activity (pg/mL/min)
Dish 10	0	0.00	180.7
	5	1.54	
	15	2.84	
	25	4.36	
	35	6.29	
Dish 11	0	0.00	110.5
	5	0.80	
	15	1.88	
	25	2.59	
	35	3.86	
Dish 12	0	0.00	142.7
	5	0.92	
	15	2.08	
	25	3.39	
	35	5.12	

 doi:10.20944/preprints202603.1833.v1

Replicate group	Time (min)	Concentration of 12-hydroxylauric acid after background subtraction (ng/mL)	Enzyme activity (pg/mL/min)
Dish 13	0	0.00	83.7
	5	0.91	
	15	1.51	
	25	1.97	
	35	2.84	
Dish 14	0	0.00	106.8
	5	0.62	
	15	1.53	
	25	3.03	
	35	3.50	
Dish 15	0	0.00	106.1
	5	0.88	
	15	1.68	
	25	2.49	
	35	3.74	

Note 2: The cell passage used in dishes 10 to 12 was P16, and the virus batch was V2. The cell passage used in dishes 13 to 15 was P15, and the virus batch was V3.

2.4.4. Linearity and Range

After linear regression was performed separately on each experimental group, the R2 value was obtained, with an average value±standard deviation of 0.9915±0.0073. As shown in Table 8, the LC-MS/MS method had good linearity. The calibration curve covered a concentration range of 0.5-100 ng/mL.

Table 8. Linearity evaluation results.

Replicate	R^2
Dish 1	0.9996
Dish 2	0.9996
Dish 3	0.9998
Dish 4	0.9871
Dish 5	0.9951
Dish 6	0.9756
Dish 7	0.9905
Dish 8	0.9853
Dish 9	0.9909
Dish 10	0.9935
Dish 11	0.9945
Dish 12	0.9978
Dish 13	0.9781
Dish 14	0.9918
Dish 15	0.9934

2.4.5. Durability

The impact of different cell passages and rAAV-hCYP4V2 batches on enzyme activity measurement was evaluated in combination with precision testing. Data from the first to ninth cell culture dishes in the precision assessment were statistically analyzed, covering three HeLa-AAVR cell passages (P16, P20, and P19). The calculated enzyme activity was 130.2±54.83 pg/mL/min, with

 doi:10.20944/preprints202603.1833.v1

an RSD of 42.11%. Data from the seventh to fifteenth cell culture dishes in the precision assessment were statistically analyzed, encompassing three rAAV-hCYP4V2 batches (V1, V2, and V3). The calculated enzyme activity was 141.3±40.19 pg/mL/min, with an RSD of 28.44%.

After completion of the enzyme reaction, the product concentration was measured immediately and again after storage at -80 ℃ for 4 weeks. The ratio of enzyme activity measured after 4 weeks of storage to that measured immediately was calculated as the recovery rate, and the value was used to evaluate stability. As shown in Table 9, enzyme activity recovery rates of 101.8%, 111.3%, and 92.2% were obtained, indicating good stability of the method and the samples.

Table 9. Stability evaluation results.

Replicate	Time (min)	Concentration of 12-hydroxylauric acid (ng/mL)	Enzyme activity (pg/mL/min)	Re-measured values after four weeks	Enzyme activity (pg/mL/min)	Enzyme activity recovery rate (%)
Dish 4	0	BQL[3]	67.2	BQL	68.4	101.8
	5	BQL		0.64		
	15	0.95		1.12		
	25	1.66		1.6		
	35	2.44		2.39		
Dish 5	0	BQL	52.0	BQL	57.9	111.3
	5	0.52		0.56		
	15	0.85		0.91		
	25	1.19		1.24		
	35	1.83		2.12		
Dish 6	0	BQL	60.0	BQL	55.3	92.2
	5	0.51		0.52		
	15	0.82		0.96		
	25	1.39		1.28		
	35	2.18		1.92		

Note 3: BQL indicated values below the quantification limit.

2.5. Practical Application of the Established Method

To evaluate the feasibility of the established method in practical applications, it was applied to determine the enzyme activity of three rAAV-hCYP4V2 products. As shown in Table 10, CYP4V2 enzyme activity was successfully detected in all three products, demonstrating that the method can be applied to different serotype vectors. Specifically, the average enzyme activity of the rAAV8-hCYP4V2 product was 328.4 ± 78.51 pg·mL-1·min-1 (RSD = 23.91%). The average enzyme activity of the rAAV2-hCYP4V2 product was 150.7 ± 24.26 pg·mL-1·min-1 (RSD = 16.10%), indicating excellent repeatability. The enzyme activity of the hybrid serotype product rAAV2/8-hCYP4V2 was 159.7 ± 34.39 pg·mL-1·min-1 (RSD = 21.53%).

 doi:10.20944/preprints202603.1833.v1

Table 10[4]. The application results of the established method.

Product	Average enzyme activity ($pg \cdot mL^{-1} \cdot min^{-1}$)	Standard deviation	RSD (%)
rAAV8-hCYP4V2	328.4	78.51	23.91
rAAV2-hCYP4V2	150.7	24.26	16.10
rAAV2/8-hCYP4V2	159.7	34.39	21.53

Note 4: All data are based on 3 independent replicates.

3. Discussion

The LC-MS/MS method established in this study achieves, for the first time, direct and absolute quantification of CYP4V2 enzyme activity in rAAV-hCYP4V2 gene therapy products. Compared with traditional fluorescence- or immunology-based methods, this approach offers higher specificity and sensitivity and effectively minimizes matrix interference, making it suitable for detecting enzymes expressed at low levels. Through systematic optimization of the cell model (HeLa-AAVR+HU pre-treatment), transduction conditions (MOI = 3×10^5, cell number = 3×10^6), and the enzymatic reaction system (coenzyme saturation conditions), the robustness and repeatability of the detection were significantly improved.

Verification results demonstrated that the method has good linearity over the range of 0.5-100 ng/mL, with high accuracy (average recovery rate of 100.6%), and that its precision meets the requirements of biological analytical methods. The intra-batch relative standard deviation (RSD≤47.8%) falls within the commonly accepted range for biological activity assays, primarily due to inherent variability associated with cell-based experiments. Unlike chemical analyses, enzyme activity measured using this method is directly affected by multiple biological factors, such as virus transduction efficiency, cell status and passage number, lysis homogeneity, and fluctuations in expression and function of the target enzyme. Therefore, the observed intra-batch variation reflects not only errors in the analysis process but also the inherent fluctuations of complex biological processes from living cells to functional proteins. Nevertheless, the method demonstrates good reproducibility (intermediate precision RSD≤28.4%) across different operators and virus batches, which indicates that it can provide a reliable and repeatable quantitative assessment of AAV-hCYP4V2 biological activity under strict control of key experimental variables.

Compared with fluorescent substrate-based CYP450 activity assay reported in the literature[15], this method does not require a derivatization and can enable specific mass spectrometry-based detection in MRM mode, effectively avoiding interference from endogenous fluorescence. Furthermore, the introduction of an exogenous coenzyme system helps overcome issues related to poor substrate accessibility, thereby enhancing the reaction efficiency.

This method was successfully applied to determine the enzyme activity of AAV2, AAV8 and AAV2/8 mixed serotype products, indicative of its broad applicability. In future studies, this method may be extended to evaluate the activity of other CYP4V2 mutant types or vector systems. This study primarily focuses on in vitro cell lysate-based systems. Although LC-MS/MS has high sensitivity, its automation in clinical trials remains limited, partly due to the complexity of sample pretreatment.[16] Future work may explore the application of this method to in vivo tissue samples or clinical blood samples. In addition, automation and adaptation of the method for high-throughput analysis represent important directions for future improvement.

 doi:10.20944/preprints202603.1833.v1

4. Materials and Methods

4.1. Main Instruments

LC-MS/MS analysis was performed using a Shimadzu LMS-8050 triple quadrupole mass spectrometer equipped with a Nexera X2 ultra-high-performance liquid chromatograph. Cell culture was conducted in a BIOBASE QP-160 carbon dioxide incubator.

4.2. Key Reagents

Lauric acid and its hydroxylated metabolite (12-hydroxydodecanoic acid) were purchased from Macklin. Tolbutamide (used as the internal standard for liquid chromatography) was purchased from Solarbio. Recombinant human cytochrome P450 oxidoreductase (POR) was purchased from R&D Systems. Human cytochrome b5 and hydroxyurea were purchased from Sigma-Aldrich. Reduced coenzyme II (NADPH) tetrasodium salt was purchased from Sangon Biotech (Shanghai) Co., Ltd. DMEM basal medium for cell culture, fetal bovine serum, PBS, trypsin-EDTA, and penicillin-streptomycin were purchased from Gibco. The BCA protein assay kit was purchased from Yeasen Biotechnology (Shanghai) Co., Ltd. LC-MS grade acetonitrile and methanol were purchased from Fisher Scientific. Chromatographically pure ethyl acetate and acetic acid were purchased from DIKMA.

4.3. Virus

Virus samples of rAAV2-hCYP4V2, rAAV8-hCYP4V2 and rAAV2/8-hCYP4V2 were obtained from retained samples of the National Institutes for Food and Drug Control (NIFDC).

4.4. Methods

Lauric acid (dodecanoic acid), a representative medium- to long-chain fatty acid, was subjected to ω-hydroxylation, a typical catalytic reaction of the CYP4V2 enzyme.[17,18] This reaction relies on the electron transfer mediated by cytochrome P450 reductase (POR)[19–22] and cytochrome b5[23–26], as well as the reducing equivalent donor β-nicotinamide adenine dinucleotide phosphate (NADPH)[27,28]. Therefore, recombinant human POR and human cytochrome b5 were exogenously added to the cell lysate to ensure a maximum reaction rate and accurately reflect CYP4V2 functional activity. The standard procedure is as follows: HeLa AAVR cells were pretreated with 0.5 mM hydroxyurea for 24 h, seeded at a density of 3×10^6 cells/dish, and then transduced with rAAV-hCYP4V2 at MOI=3×10^5 for 120 h. Cells were collected and resuspended in 1 mL of potassium phosphate buffer per 10 cm cell culture dish, followed by ultrasonication. The lysate was then diluted to a final volume of 2 mL. In a 250 μL reaction system, 200 μL of cell lysate, P450 reductase (final concentration 40 nM), cytochrome b5 (final concentration 20 nM), and lauric acid substrate (final concentration 250 μM) were added. After incubation at 37 °C for 2 min, NADPH (final concentration 1 mM) was added to initiate the reaction. Reaction times were precisely controlled at 0, 5, 15, 25, and 35 min. Then, 1 M H_2SO_4 was added to terminate the reaction, and the samples were stored at -80 °C. During sample pretreatment, 200 μL of the terminated reaction solution was added with the internal standard. Standard curve and quality control samples were prepared in parallel using blank cell lysate. All samples were subjected to liquid-liquid extraction with ethyl acetate, nitrogen evaporation at 40 °C, and reconstitution in 30% methanol-water before analysis. The concentration of 12-hydroxylauric acid in the samples was determined using the internal standard method. Enzyme activity was expressed as the amount of product generated per unit time and volume (pg/mL/min), with the background value at 0 min subtracted.

The LC-MS/MS parameters were set as follows. Liquid chromatography conditions were as follows: mobile phase A, 0.1% acetic acid aqueous solution; mobile phase B, acetonitrile; flow rate, 0.3 mL/min; column temperature, 40 °C; injection volume, 5 μL; and chromatographic column, ACE Excel 3 super C18 (particle size: 3 μm, 100 mm×2.1 mm). Mass spectrometry parameters were as

 doi:10.20944/preprints202603.1833.v1

follows: ion source, electrospray; scanning mode, negative ion; detection mode, MRM; spray voltage, -3.0 kV; nebulizing gas flow rate, 3.0 L/min; drying gas flow rate, 10.0 L/min; heating gas flow rate, 10.0 L/min; desolvation line temperature, 250 °C; heating block temperature, 400 °C; interface temperature, 300 °C; ion source interface, Turbo IonSpray (ESI); ionization mode, negative ion; and data acquisition time, 11 min. MRM transitions were optimized for precursor/product ion pairs, and collision energy and other compound-specific parameters were adjusted accordingly. The optimized MRM transitions and conditions are shown in Table 11.

Table 11. Ion-pair parameters of 12-hydroxylauric acid and tolbutamide.

No.	Compound name	Precursor ion	Product ion	Q1 Pre Bias (V)	CE	Q3 Pre Bias (V)
1	12-Hydroxylauric acid	215.3	169.3*	10	18	18
			197.2	15	17	20
2	Tolbutamide	269	170.1	28	18	18

4.5. Methodology Validation

4.5.1. Specificity

Three groups were established: a blank control group without rAAV-hCYP4V2 transduction, a substrate control group containing the enzyme reaction substrate following rAAV-hCYP4V2 transduction, and a positive group. Each group was subjected to three independent enzyme activity reaction runs.

4.5.2. Accuracy

The accuracy of LC-MS/MS detection was evaluated. Following rAAV-hCYP4V2 transduction, the enzymatic activity assay was performed. After the enzymatic activity reaction was terminated, 100 μL of samples was collected at three time points and mixed with equal volumes of low-, medium-, and high-level quality control samples to determine the concentrations of 12-hydroxylauric acid and compare it with the theoretical concentration.

4.5.3. Precision

Repeatability was defined as six replicate measurements performed under the same operator within a fixed period according to the standard operating procedure, with RSD values calculated from the measured six enzyme activities.

Intermediate precision was assessed by measuring enzyme activity from three different virus batches analyzed by two operators at different times, with RSD values calculated accordingly.

4.5.4. Linearity and Range

According to the standard operating procedure, enzymatic reaction time points were used as the x-axis, and the 12-hydroxy-octadecanoic acid concentration measured by LC-MS/MS was used as the y-axis. Linear regression was performed using three replicates to evaluate the assay linearity. The analytical range corresponded to the LC-MS/MS calibration curve (0.5-100 ng/mL), covering the detection requirements of this method.

4.5.5. Durability

The effects of different cell passages and different rAAV-hCYP4V2 batches on enzyme activity measurement were evaluated. Meanwhile, the stability of test samples stored at -80 °C for 4 weeks after completion of the enzymatic reaction was evaluated.

 doi:10.20944/preprints202603.1833.v1

4.6. Application of Methods

To verify the applicability of the established method and its ability to distinguish differences in activities of different products, the method was applied in the quantitative analysis of CYP4V2 enzyme activity in three rAAV-hCYP4V2 gene therapy products, including an AAV8 serotype vector (rAAV8-hCYP4V2), an AAV2 serotype vector (rAAV2-hCYP4V2), and a hybrid serotype research product (rAAV2/8-hCYP4V2). All products were tested according to the standard operating procedures described in Section 2.4, with three independent replicates (n=3) for each product. By comparing mean enzyme activity, coefficient of variation (RSD), and statistical differences among products, the applicability of the method for product quality control and comparative analysis was evaluated.

4.7. Data Processing and Statistical Analysis

All validation experiments were independently conducted at least three times to ensure data reliability (n≥3). Data are expressed as mean ± standard deviation (mean ± SD).

Enzyme activity calculation: The enzyme activity of CYP4V2 was determined based on the production rate of its enzymatic reaction product, 12-hydroxylauric acid. The calculation of the net product formation over a defined time interval was performed by subtracting the background value at the zero time point (t_0) from the product concentration measured at a specific time point (t). Enzyme activity was expressed as the amount of product per unit volume per unit time (pg/mL/min).

Standard curve and chromatographic analysis: LabSolutions software was used to perform a weighted least-squares linear regression on the analyte's theoretical concentration against the ratio of the analyte peak area to that of the internal standard. The weight factor was $1/x^2$. The analyte concentration in each sample was calculated using the obtained regression equation. Statistical calculations were carried out using Microsoft Office Excel 2013.

Methodological validation index analysis: The established analytical method was validated. Precision, including repeatability, was evaluated based on the relative standard deviation (RSD), which was calculated using the following formula: RSD (%) = (standard deviation/mean) ×100%.

Statistical analysis and data visualization: All statistical analyses and graphical representations were carried out using GraphPad Prism 10.1.2 software.

Author Contributions: Conceptualization, Chenggang Liang and Yong Zhou; methodology, Ge Ren; software, Xi Qin and Wenjing Luo; validation, Ge Ren, Yiran Li and Yanrong Cao; formal analysis, Xi Qin and Wenjing Luo; writing—original draft preparation, Ge Ren; writing—review and editing, Yong Zhou; supervision, Chenggang Liang. All authors have read and agreed to the published version of the manuscript.

Funding: This research was funded by Beijing Municipal Science and Technology Project, grant number Z251100004625002, and the National Key R&D Program of China, grant number 2023YFC3403305.

Informed Consent Statement: Not applicable.

Data Availability Statement: The data presented in this study are available on reasonable request from the first author.

Acknowledgments: We would like to thank Shimadzu (China) Co., Ltd. (Beijing) for providing instrument support and technical assistance during this study.

Conflicts of Interest: The authors declare no conflicts of interest.

Abbreviations

The following abbreviations are used in this manuscript:

AAV	Adeno-associated virus
BCA	Bicinchoninic acid assay
BCD	Bietti crystalline dystrophy
BQL	Below the quantification limit

 doi:10.20944/preprints202603.1833.v1

CE	Collision energy
CYP4V2	Cytochrome P450 family 4 subfamily V member 2
DMEM	Dulbecco's Modified Eagle Medium
EDTA	Ethylenediaminetetraacetic acid
ESI	Electrospray ionization
HPLC	High-performance liquid chromatography
HU	Hydroxyurea
ICH	International Council for Harmonisation
LC-MS/MS	Liquid chromatography-tandem mass spectrometry
LLOQ	Lower limit of quantification
MOI	Multiplicity of infection
MRM	Multiple reaction monitoring
NADPH	Nicotinamide adenine dinucleotide phosphate (reduced form)
NIFDC	National Institutes for Food and Drug Control
PBS	Phosphate-buffered saline
POR	Cytochrome P450 oxidoreductase
Q1 Pre Bias	Quadrupole 1 pre-bias
Q3 Pre Bias	Quadrupole 3 pre-bias
R^2	Coefficient of determination
rAAV-hCYP4V2	Recombinant adeno-associated virus carrying the human *CYP4V2* gene
RPE	Retinal pigment epithelium
RSD	Relative standard deviation
SD	Standard deviation

References

1. Shen, C.; Yang, Q.; Chen, K.; Ma, H.; Wang, X.; Tong, J.; Shen, Y.; Cui, H. Uncovering the Role of Ferroptosis in Bietti Crystalline Dystrophy and Potential Therapeutic Strategies. *Cell Commun Signal* **2024**, *22*, 359, doi:10.1186/s12964-024-01710-x.
2. Chen, X.; Liu, X.; Cui, S.; Wang, G.; Liu, Y.; Qu, G.; Jiang, L.; Liu, Y.; Li, X. Safety and Vision Outcomes Following Gene Therapy for Bietti Crystalline Dystrophy: A Nonrandomized Clinical Trial. *JAMA Ophthalmol* **2025**, *143*, 126, doi:10.1001/jamaophthalmol.2024.5619.
3. Meng, X.; Jia, R.; Zhao, X.; Zhang, F.; Chen, S.; Yu, S.; Liu, X.; Dou, H.; Feng, X.; Zhang, J.; et al. In Vivo Genome Editing via CRISPR/Cas9-Mediated Homology-Independent Targeted Integration for Bietti Crystalline Corneoretinal Dystrophy Treatment. *Nat Commun* **2024**, *15*, 3773, doi:10.1038/s41467-024-48092-9.
4. Jia, R.; Chen, S.; Li, W.; Zhang, J.; Qu, B.; Qiao, J.; Meng, X.; Yu, S.; Liu, X.; Xu, B.; et al. Unravelling CYP4V2: Clinical Features, Genetic Insights, Pathogenic Mechanisms and Therapeutic Strategies in Bietti Crystalline Corneoretinal Dystrophy. *Progress in Retinal and Eye Research* **2025**, *107*, 101377, doi:10.1016/j.preteyeres.2025.101377.
5. Yang, X.; Yin, S.; Wang, J.; Zhang, H.; Liang, C.; Luo, J.; Zhao, S.; Wei, W. Comprehensive Genotypic and Phenotypic Analysis of Bietti Crystalline Dystrophy: Insights from a Large Cohort Study. *Sci. China Life Sci.* **2025**, *68*, 3367–3378, doi:10.1007/s11427-024-2812-2.
6. Leahy, C.; Osborne, N.; Shirota, L.; Rote, P.; Lee, Y.-K.; Song, B.-J.; Yin, L.; Zhang, Y.; Garcia, V.; Hardwick, J.P. The Fatty Acid Omega Hydroxylase Genes (CYP4 Family) in the Progression of Metabolic Dysfunction-Associated Steatotic Liver Disease (MASLD): An RNA Sequence Database Analysis and Review. *Biochemical Pharmacology* **2024**, *228*, 116241, doi:10.1016/j.bcp.2024.116241.
7. Osborne, N.; Leahy, C.; Lee, Y.-K.; Rote, P.; Song, B.-J.; Hardwick, J.P. CYP4V2 Fatty Acid Omega Hydroxylase, a Druggable Target for the Treatment of Metabolic Associated Fatty Liver Disease (MAFLD). *Biochemical Pharmacology* **2022**, *195*, 114841, doi:10.1016/j.bcp.2021.114841.
8. Wang, J.; Zhang, J.; Yu, S.; Li, H.; Chen, S.; Luo, J.; Wang, H.; Guan, Y.; Zhang, H.; Yin, S.; et al. Gene Replacement Therapy in Bietti Crystalline Corneoretinal Dystrophy: An Open-Label, Single-Arm, Exploratory Trial. *Sig Transduct Target Ther* **2024**, *9*, 95, doi:10.1038/s41392-024-01806-3.
9. Trapani, I. Adeno-Associated Viral Vectors as a Tool for Large Gene Delivery to the Retina. *Genes* **2019**, *10*, 287, doi:10.3390/genes10040287.

 doi:10.20944/preprints202603.1833.v1

10. Luo, W.; Guo, L.; Lu, L.; Huang, N.; Tao, Y.; Zhang, Y.; Cao, Y.; Tian, S.-S.; Zhao, X.; Zhu, X. Preclinical Studies of an AAV8-CYP4V2 Gene Therapy VGR-R01 for the Treatment of Bietti Crystalline Dystrophy. *Mol Ther Methods Clin Dev* **2025**, *33*, 101460, doi:10.1016/j.omtm.2025.101460.
11. Li, Z.-P.; Shi, Y.-F.; Hou, L.-H.; Jin, P.-F.; Ma, S.-H.; Pan, H.-X.; Zhang, J.-L.; Shan, Y.-M.; Huang, H.-T.; Wu, S.-P.; et al. Batch-to-Batch Consistency Trial of an Adenovirus Type-5 Vector-Based COVID-19 Vaccine in Adults Aged 18 Years and Above. *Expert Review of Vaccines* **2022**, *21*, 1843–1849, doi:10.1080/14760584.2022.2119133.
12. Noort, K.J.; Santobuono, M.; D'Amico, E.; Chan, W.S.; Short, S.; Selck, H.; Spurgeon, D.J. In Vivo Measurement of Xenobiotic Detoxification in Annelids: ECOD Activity in a Terrestrial, a Freshwater, and an Estuarine Worm. *Ecotoxicology and Environmental Safety* **2025**, *307*, 119411, doi:10.1016/j.ecoenv.2025.119411.
13. Li, M.; Nawa, Y.; Ishida, S.; Kanda, Y.; Fujita, S.; Fujita, K. Label-Free Chemical Imaging of Cytochrome P450 Activity by Raman Microscopy. *Commun Biol* **2022**, *5*, 778, doi:10.1038/s42003-022-03713-1.
14. Ács, A.; Kovács, A.W.; Győri, J.; Farkas, A. Optimization of Assay Conditions to Quantify ECOD Activity in Vivo in Individual Daphnia Magna. Assay Performance Evaluation with Model CYP 450 Inducers/Inhibitors. *Ecotoxicology and Environmental Safety* **2024**, *273*, 116159, doi:10.1016/j.ecoenv.2024.116159.
15. Juvonen, R.O.; Ahinko, M.; Huuskonen, J.; Raunio, H.; Pentikäinen, O.T. Development of New Coumarin-Based Profluorescent Substrates for Human Cytochrome P450 Enzymes. *Xenobiotica* **2019**, *49*, 1015–1024, doi:10.1080/00498254.2018.1530399.
16. Suarez-Amaran, L.; Song, L.; Tretiakova, A.P.; Mikhail, S.A.; Samulski, R.J. AAV Vector Development, Back to the Future. *Molecular Therapy* **2025**, *33*, 1903–1936, doi:10.1016/j.ymthe.2025.03.064.
17. Choi, Y.J.; Zhou, Y.; Lee, J.-Y.; Ryu, C.S.; Kim, Y.H.; Lee, K.; Kim, S.K. Cytochrome P450 4A11 Inhibition Assays Based on Characterization of Lauric Acid Metabolites. *Food and Chemical Toxicology* **2018**, *112*, 205–215, doi:10.1016/j.fct.2017.12.063.
18. Jarrar, Y.B.; Shin, J.; Lee, S. Identification and Functional Characterization of CYP4V2 Genetic Variants Exhibiting Decreased Activity of Lauric Acid Metabolism. *Annals of Human Genetics* **2020**, *84*, 400–411, doi:10.1111/ahg.12388.
19. Uehara, S.; Iida, Y.; Ida-Tanaka, M.; Goto, M.; Kawai, K.; Yamamoto, M.; Higuchi, Y.; Ito, S.; Takahashi, R.; Kamimura, H.; et al. Humanized Liver TK-NOG Mice with Functional Deletion of Hepatic Murine Cytochrome P450s as a Model for Studying Human Drug Metabolism. *Sci Rep* **2022**, *12*, 14907, doi:10.1038/s41598-022-19242-0.
20. Velazquez, M.N.R.; Parween, S.; Udhane, S.S.; Pandey, A.V. Variability in Human Drug Metabolizing Cytochrome P450 CYP2C9, CYP2C19 and CYP3A5 Activities Caused by Genetic Variations in Cytochrome P450 Oxidoreductase. *Biochemical and Biophysical Research Communications* **2019**, *515*, 133–138, doi:10.1016/j.bbrc.2019.05.127.
21. Rojas Velazquez, M.N.; Therkelsen, S.; Pandey, A.V. Exploring Novel Variants of the Cytochrome P450 Reductase Gene (POR) from the Genome Aggregation Database by Integrating Bioinformatic Tools and Functional Assays. *Biomolecules* **2023**, *13*, 1728, doi:10.3390/biom13121728.
22. Bapiro, T.E.; Martin, S.; Blacker, T.S.; Wilkinson, S.D.; Orton, A.L.; Hariparsad, N.; Jones, R.D.O.; Duchen, M.R.; Harlfinger, S. A Mismatch in Enzyme-Redox Partnerships Underlies Divergent Cytochrome P450 Activities between Human Hepatocytes and Microsomes. *Commun Biol* **2025**, *8*, 1539, doi:10.1038/s42003-025-08903-1.
23. Pearl, N.M.; Wilcoxen, J.; Im, S.; Kunz, R.; Darty, J.; Britt, R.D.; Ragsdale, S.W.; Waskell, L. Protonation of the Hydroperoxo Intermediate of Cytochrome P450 2B4 Is Slower in the Presence of Cytochrome P450 Reductase Than in the Presence of Cytochrome B5. *Biochemistry* **2016**, *55*, 6558–6567, doi:10.1021/acs.biochem.6b00996.
24. Yoo, S.-E.; Yi, M.; Kim, W.-Y.; Cho, S.-A.; Lee, S.S.; Lee, S.-J.; Shin, J.-G. Influences of Cytochrome B5 Expression and Its Genetic Variant on the Activity of CYP2C9, CYP2C19 and CYP3A4. *Drug Metabolism and Pharmacokinetics* **2019**, *34*, 201–208, doi:10.1016/j.dmpk.2019.03.001.

 doi:10.20944/preprints202603.1833.v1

25. Esteves, F.; Campelo, D.; Urban, P.; Bozonnet, S.; Lautier, T.; Rueff, J.; Truan, G.; Kranendonk, M. Human Cytochrome P450 Expression in Bacteria: Whole-Cell High-Throughput Activity Assay for CYP1A2, 2A6 and 3A4. *Biochemical Pharmacology* **2018**, *158*, 134–140, doi:10.1016/j.bcp.2018.10.006.
26. Stiborová, M.; Indra, R.; Moserová, M.; Frei, E.; Schmeiser, H.H.; Kopka, K.; Philips, D.H.; Arlt, V.M. NADH:Cytochrome b_5 Reductase and Cytochrome b_5 Can Act as Sole Electron Donors to Human Cytochrome P450 1A1-Mediated Oxidation and DNA Adduct Formation by Benzo[*a*]Pyrene. *Chem. Res. Toxicol.* **2016**, *29*, 1325–1334, doi:10.1021/acs.chemrestox.6b00143.
27. Schulz, C.; Kammerer, S.; Küpper, J.-H. NADPH-Cytochrome P450 Reductase Expression and Enzymatic Activity in Primary-like Human Hepatocytes and HepG2 Cells for in Vitro Biotransformation Studies. *CH* **2019**, *73*, 249–260, doi:10.3233/CH-199226.
28. Iqbal, T.; Das, D. Biochemical Investigation of Membrane-Bound Cytochrome B5 and the Catalytic Domain of Cytochrome B5 Reductase from *Arabidopsis Thaliana*. *Biochemistry* **2022**, *61*, 909–921, doi:10.1021/acs.biochem.2c00002.